

Thermal curing and degradation kinetics of terpolymer resins derived from vanillin oxime, formaldehyde and p-chloro-/p-methylacetophenone

Narendra Pal Singh Chauhan[†]

Department of Chemistry, B. N. P. G. College, Udaipur - 313001, Rajasthan, India

(Received 5 June 2014 • accepted 10 August 2014)

Abstract—A novel class of linear terpolymer resins have been prepared from various macromers formed by vanillin oxime (VO), formaldehyde (F) and p-chloro/p-methylacetophenone in the presence of an acid as catalyst by convenient polycondensation process. The conversion of different macromers into respective terpolymeric resin was studied by DSC analysis from -50°C to 250°C . The first thermal transition endotherms ranging from $108\text{--}137^{\circ}\text{C}$ (VOFCA) and $125\text{--}150^{\circ}\text{C}$ (VOFMA) are due to expulsion of water molecules, and the second thermal transition exotherms $177\text{--}247^{\circ}\text{C}$ (VOFCA) and $183.9\text{--}249.8^{\circ}\text{C}$ (VOFMA) are attributed to the formation of methylene linkage between macromers moieties by utilizing methanol groups at terminals. The activation energy required for conversion of methanol into methylene groups for VOFCA and VOFMA was 3.4 and 3.9 kJ/mol, respectively. Structural confirmations were determined through IR, UV-Vis, ^1H NMR spectroscopy and GPC data. The activation energy (E_a) and thermodynamic parameters of the thermal decomposition process were investigated with thermogravimetric analysis (TGA) by isoconversional integral Kissinger-Akahira-Sunose (KAS) and differential Friedman methods. Empirical kinetic models, as well as generalized master plots, were applied to explain the degradation mechanisms of terpolymer resins. The degradation reaction follows Avrami-Erofeev (nucleation and growth) at initial stage to Jander (three-dimensional diffusion) model for PVOMAF and Jander (two-dimensional diffusion) for PVOFCA governed mechanisms. Among all the tested terpolymers, both resins revealed better activity compared to standard drugs as Gentamycin, Amphotericin, Chloramphenicol, Ciprofloxacin and Norfloxacin.

Keywords: Polycondensation, Vanillin Oxime, TG-DTG, Characterization, Isoconversional, Kinetics, Mechanism, Antibacterial Activity

INTRODUCTION

The synthesis of new multifunctional materials that are based on renewable resources has been accepted as a strategy to contribute to a sustainable development, and that pervades our life in a variety of applications. Vanillin, which is an important aromatic flavor compound used in foods, beverages, perfumes, and pharmaceuticals [1], represents a sustainable and valuable chemical feedstock [2,3]. It is also used for other purposes such as constituent in cosmetic and drug preparations. Apart from its flavoring properties, vanillin and halo substituted acetophenone based polymers also exhibit several bioactive properties [4-6]. Biobased resins or thermosets are synthetic materials that consist partially or completely of renewable raw materials and which can no longer be melted down after a single hardening step (chemical reaction). Natural oils, carbohydrates and natural phenol compounds (such as vanillin, tannin and lignin) are generally used to develop biobased materials. Recently, a new bio-based monomer, methacrylated vanillin, and its vinyl ester resin were synthesized for polymer composite applications [7]. Polyvanillin was prepared by electrochemical reductive polymerization of divanillin in aqueous sodium hydroxide [8].

One of the most widely used techniques for studying the kinetics

of cure reaction is thermal analysis by differential scanning calorimetry (DSC) in isothermal or dynamic modes. Cure kinetic models can be classified into two categories: phenomenological and mechanistic models. Mechanistic models are made from the balance of chemical species taking part in the chemical reaction. In many cases, it is not easy to derive a mechanistic model especially when the cure reaction is very complicated. Phenomenological models, based on empirical data, proved to be more appropriate as compared to the mechanistic model.

The “model-free” isoconversional methods are widely adopted techniques for deriving relevant kinetic parameters using thermogravimetric (TG) and differential thermogravimetric (DTG) curves measured at different heating rates, which make no presumption about the reaction function and reaction order [10-12].

Generally, phenol and formaldehyde go through addition and condensation reactions under either alkaline condition to form cross-linked thermoset polymers or under acidic condition to form linear thermoplastic polymers. The structure and properties of the polymer depend highly on the reaction conditions. The inclusion of other materials, such as lignin and its derivatives, in the phenolic resin synthesis has been shown to modify thermal stability and degradation kinetics of the resulting resins [13]. Terpolymer as Lignin-phenol-formaldehyde (LPF) resin was found to have higher thermal stability under both nitrogen and air conditions than PF resins with different degradation characteristics [14]. Meanwhile, the LPF novolac resins were found to be less stable at lower tem-

[†]To whom correspondence should be addressed.

E-mail: narendrapalsingh14@gmail.com, rajveerchauhan14@gmail.com
Copyright by The Korean Institute of Chemical Engineers.

peratures than PF resins, but they were comparable to PF resins at higher temperatures [15]. On the other hand, to trace exactly the structure-property relationships for terpolymer resin system, understanding of the cure (thermal) process is essential in order to get a better control of the reactions and in consequence to optimize the physical properties of the final product. Many studies have been conducted on the curing reaction kinetics of thermosetting resins employing various techniques, experimental procedures, and data analysis methods [16].

The properties of products obtained by terpolymerization of functional monomers by polycondensation approach can be changed in a wide range, providing links to the research areas of hybrid structures and bio-related materials. The properties are influenced by the molar proportion, choice of comonomer and distribution of the functional monomer in the product.

However, relatively few studies have been reported on the thermostability and thermal degradation kinetics of the functional phenolic based terpolymers. A more detailed study would be of value for the material community because the terpolymer must encounter elevated temperatures at almost every step in the manufacturing, compounding, and processing steps as well as in service and during repair.

Recently, our research group synthesized functionalized terpolymers derived from various oxime based monomers as p-acetylpyridine oxime, p-chloroacetophenone oxime and 8-hydroxy quinoline with chloro-/methoxy-/methyl substituted acetophenone by using formaldehyde as condensing unit, which has applications ranging from electronic devices to biological materials. These terpolymers have been found to be an excellent antimicrobial agent and also with good thermal stability [17-20].

In view of the need for renewable resources based ecofriendly antimicrobial finishing, this research has focused on the synthesis of antimicrobial agents where the leaching antimicrobials have been replaced with the bound antimicrobials. I attempted to develop a resin with a recoverable antimicrobial activity based on the desorption/adsorption of cationic bactericide by the ion-exchange mechanism [21]. The aims of this study were to investigate the release kinetics of the agent and the antimicrobial activity of this newly developed terpolymer resins. In this study, vanillin oxime, formaldehyde and chloro-/methyl acetophenone are used to prepare phenolic terpolymer resin by polycondensation technique. Within these investigations, I have found that a modification of vanillin as vanillin oxime is a suitable renewable monomer for the synthesis of bio-based phenolic resins. Additionally, the thermal properties of the synthesized terpolymers were studied to learn about the properties and possible applications in biomedical applications.

EXPERIMENTAL

1. Chemicals and Reagents

Vanillin oxime was prepared by vanillin (Ranbaxy, Mumbai), and hydroxylamine hydrochloride (Merck, India) in basic medium earlier [21] 4-methylacetophenone, and 4-chloroacetophenone were obtained commercially from Sisco Research Limited, India with mass fraction purity values of 0.96 and 0.94, respectively. The samples were purified by repeated distillation under reduced pressure

before the experimental measurements. The purity of the compounds was checked by gas-liquid chromatography and from the average ratios of the mass of carbon dioxide recovered from the combustion to that calculated from the mass of sample as: 0.985370 for 4-methylacetophenone and 0.98700 for 4-chloroacetophenone. Formaldehyde (37%) (AR grade, Merck) was used as received. All other chemicals, solvent, and indicators were analytical grade procured from Thomas Baker, Mumbai, India. Double distilled water was used for all the experiments.

2. Terpolymerization

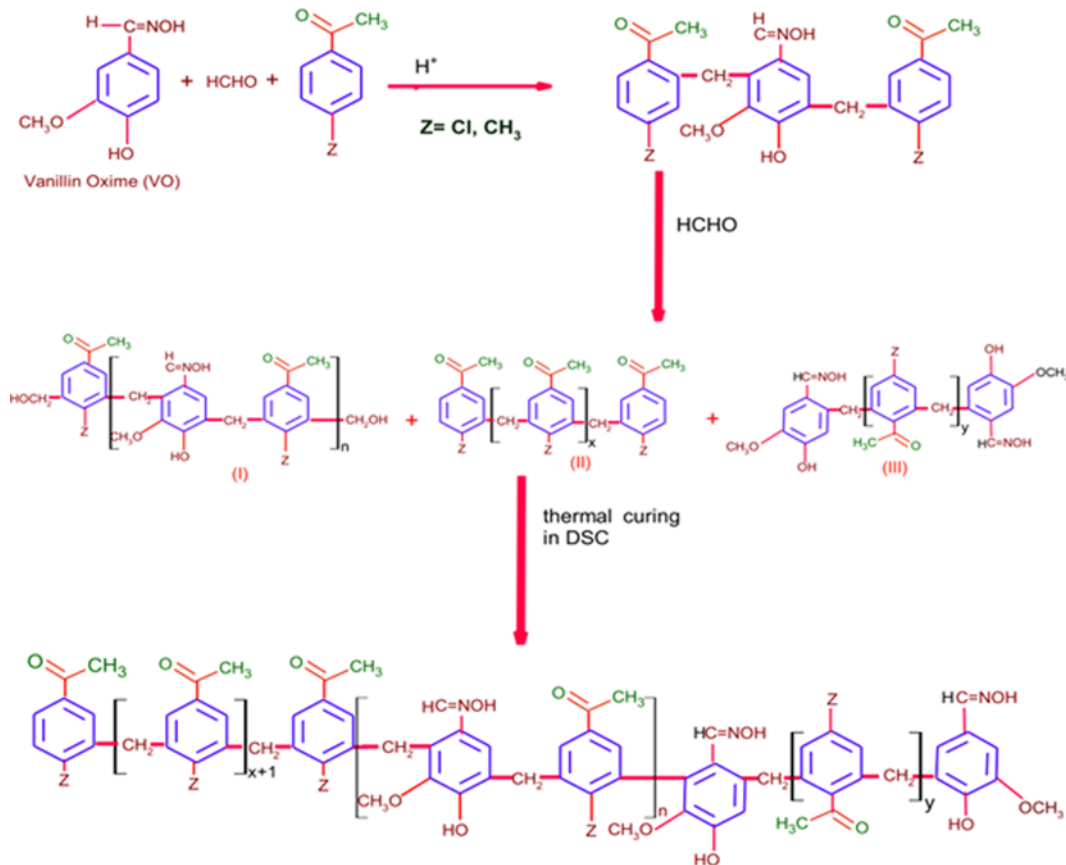
The terpolymer resin, vanillin oxime-co-formaldehyde-co-p-chloroacetophenone (PVOFCA) and vanillin oxime-co-formaldehyde-co-p-methylacetophenone (PVOFMA) were synthesized by condensing vanillin oxime (5.51 g, 0.3 mol) and p-chloroacetophenone (3.1 g, 0.2 mol) or p-methylacetophenone (2.7 g, 0.2 mol) with 37% formaldehyde (18.1 ml, 0.5 mol) in a mol ratio of 3:2:5 in the presence of 50 mL solvent (1, 4-dioxane) in 100 ml of 2 M HCl as a catalyst at $120 \pm 2^\circ\text{C}$ for 6 h in an oil bath with occasional shaking to ensure thorough mixing followed by cooling to room temperature and solvent was evaporated. Solvent was removed by distillation under reduced pressure. The viscous polymeric product was dissolved in chloroform and washed with 0.1 N NaOH solution several times, and washed with distilled water. The organic layer was dried with anhydrous Na_2SO_4 , filtered and then chloroform was evaporated. The viscous brown resinous mixture was dried under vacuum for 24 h before further analyses.

Resinous mixture may have three possibilities of different macromers of different chain length as (I) vanillin oxime-co-formaldehyde-p-chloroacetophenone with methylol groups at terminal positions, which may be responsible for crosslinking site for other macromers; (II) p-chloro/p-methylacetophenone-co-formaldehyde, and (III) vanillin oxime-co-formaldehyde. We earlier reported the possibilities of the existence of copolymer (4-chloroacetophenone oxime-co-formaldehyde) and terpolymer (4-chloroacetophenone oxime-co-formaldehyde) by taking separate experiments [22]. This strongly suggests all three possibilities of existence of (I), (II) and (III) which are shown in Scheme 1.

A study of the thermal process (post-polymerization) would provide more specific information about the structures and arrangement of different macromers in the resin system. DSC technique allows the direct determination of the rate of post-polymerization reaction, assuming that the heat produced by the curing is proportional to the number of methylol units reacted. Therefore, DSC can also be used in development of kinetic models, which represents a fundamental step for the optimization of conditions during application of the linear resin system [23]. The Kissinger method utilizes the relationship that for thermoset curing, the extent of reaction at the peak exotherm of particular degree of conversion (α_p) is constant and independent of the heating rate [24]. The activation energy E can be computed by

$$\frac{d[\ln \phi/T_p^2]}{d(1/T_p)} = -\frac{E_a}{R} \quad (1)$$

where ϕ (dT/dt) is heating rate, T_p is peak temperature, R is gas constant and E_a is activation energy. E_a can be obtained from the linear plot of $\ln \beta/T_p^2$ against $1/T_p$.



Scheme 1. Polycondensation of different macromers (prepolymer) as an intermediate into respective linear terpolymer resin.

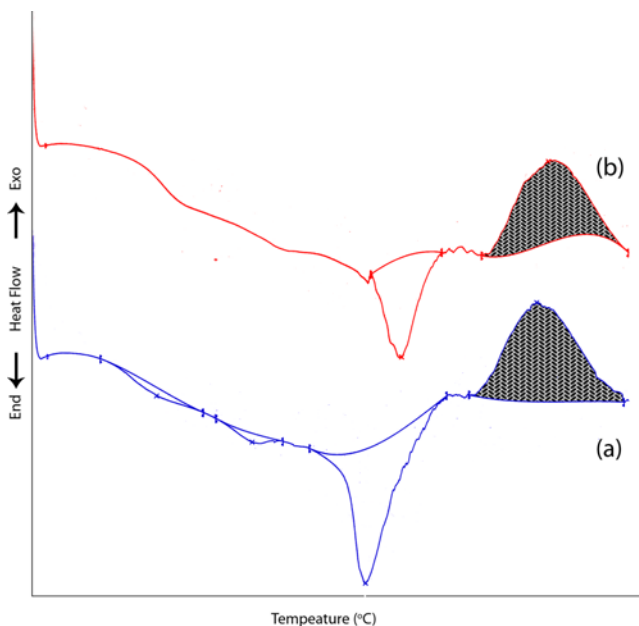


Fig. 1. DSC thermogram from -50 to 250 °C for terpolymer PVOFCA and PVOFMA.

The DSC experimental thermographs of the both terpolymers from -50 to 250 °C are presented in Fig. 2. The graphs show that in both cases the first endotherm is attributed to loss of bound or

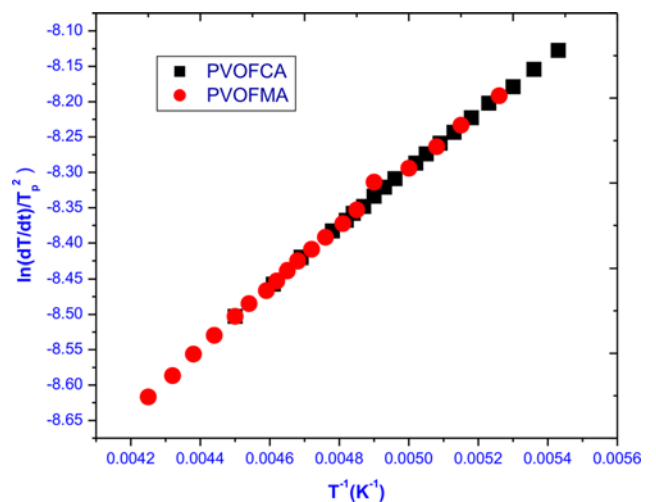


Fig. 2. Plot between $\ln(\beta/T^2)$ against $1/T$ over a wide range of conversion ($0.05 \leq \alpha \leq 0.90$) to determine cure kinetics.

free water, which is probably present in resinous mixture, and the second exotherm clearly indicates about conversion of terminal methylol groups into methylene linkage between macromer moieties, which shows curing behavior is completed in this step.

The plots between $\ln(\beta/T^2)$ against $1/T$ over a wide range of conversion ($0.05 \leq \alpha \leq 0.90$) to evaluate E_a values of both terpolymers are tabulated in Table 1 and shown in Fig. 2 The determined apparent

Table 1. DSC thermograms from -50 to 250 °C with scanning rate of 10 °C/ min

Terpolymer	Endotherm			Exotherm			
	Onset temperature T_{onset} (°C)-tendset	Peak temperature, T_p (°C)	Heat of melting (J/g)	Onset temperature T_{onset} (°C)	Peak temperature, T_p (°C)	Heat of curing (J/g)	Activation energy, E_a (kJ/mol)
PVOFCA	108.5-137.7	118.2	-30	177.6-247.5	203.8	40.6	3.4
PVOFMA	125-150	136.8	-20.7	182.9-249.9	209.4	36.2	3.9

activation energies of each thermal reaction over the range of a given conversion are 3.3 kJmol^{-1} (PVOFCA) and 3.5 kJmol^{-1} (PVOFMA).

Above results clearly indicate that during thermal reaction methylene groups are known to act as a crosslinker upon heating by creation of methylene linkage between (I), (II), and (III) and which ultimately make a linear resin system (Scheme 1).

3. Characterization

Uv-visible spectra of terpolymer resins were recorded in DMSO (spectroscopic grade) on a Shimadzu double beam spectrophotometer in the range of 200 to 450. The infrared (FT-IR) spectrum for identifying the linkages and functional groups was recorded at the frequency range of $4,000\text{-}400 \text{ cm}^{-1}$ on Perkin-Elmer 2000 FT-IR spectrometer at Sophisticated Analytical Instrumentation Facility (SAIF), Punjab University; Chandigarh. A nuclear magnetic resonance (NMR) spectrum of newly synthesized polymer resin was scanned on FT-NMR-Cryo-magnet 400 MHz (Bruker) spectrometer using DMSO- d_6 at sophisticated Analytical Instrumentation Facility Punjab University, Chandigarh. Intrinsic viscosity (η) was measured in DMSO at 30 °C using a Ubbelohde suspended level capillary viscometer. The relative and specific viscosities were measured at five concentrations in the range (0.002 to 0.010 g/ml). The value of η was determined by extrapolating the reduced and inherent viscosities to infinite dilution. The average molecular weight and its polydispersity index were determined with gel permeation chromatography (GPC) analysis. It was performed with a set up consisting of a Waters 600 pumps and 2 ultra styragel columns (10^4 , 500 \AA) with THF as the eluent at a flow rate of 1 mL/min equipped with Waters differential refractometer and calibrated with the standard linear PSt. Differential scanning calorimetry (DSC) curves were recorded with a Mettler Toledo DSC-2007 apparatus. A sample was heated from -50 to 250 °C with a heating rate of 10 °C/min under nitrogen atmosphere. Thermal gravimetric analysis (TGA) was carried out using a Mettler Toledo Star System AG 2007 Module. The results were acquired with heating rates of 10, 20, 30, and 40 °C/min under nitrogen gas from 30 to 600 °C at constant flow rate of 80 mL/min. The purpose of this study is to provide trustworthy kinetic data for prolonging life time estimation.

Non-isothermal decomposition kinetics by TGA

Kissinger-Akahira-Sunose (K-A-S) method: This method is an integral isoconversational method:

$$\ln \frac{\beta}{T^2} = \log \left(\frac{AR}{F(\alpha)E_a} \right) - \frac{E_a}{RT} \quad (2)$$

The dependence of $\ln(\beta/T^2)$ on $1/T$, calculated for the same α values at the different heating rates β can be used to calculate the activation energy.

Friedman method: The Friedman method, which is the most widely used method for kinetic analysis, is used to study the thermal properties of the polymer and the principle is shown as:

$$\ln \left(\beta \frac{d\alpha}{dT} \right) = \ln [A \cdot f(\alpha)] - \frac{E_a}{RT} \quad (3)$$

Criado method for determination of reaction mechanism: The Criado method [19] defines a function

$$z(\alpha) = \frac{d\alpha/dt}{\beta} \pi(x) T \quad (4)$$

where $x = E/RT$; and $\pi(x)$ is an approximation of the temperature integral which cannot be expressed in a simple analytical form. Similarly,

$$z(\alpha) = f(\alpha) \cdot g(\alpha) \quad (5)$$

This last equation was used to obtain the master curves as a function of the reaction degree corresponding to different models already reported in our previous reported work.

Plotting the $z(\alpha)$ function calculated using experimental data using Eq. (4), and comparing with the master curves leads to easy and precise determination of the mechanism of a solid state process. Activation energy, E_a , was calculated by fitting the K-A-S equation to temperature and heating rates value at $10 \text{ °C} \cdot \text{min}^{-1}$ for a given conversion value (α). This E_a is called 'apparent activation energy' because it is the sum of chemical reaction and physical process in thermal degradation.

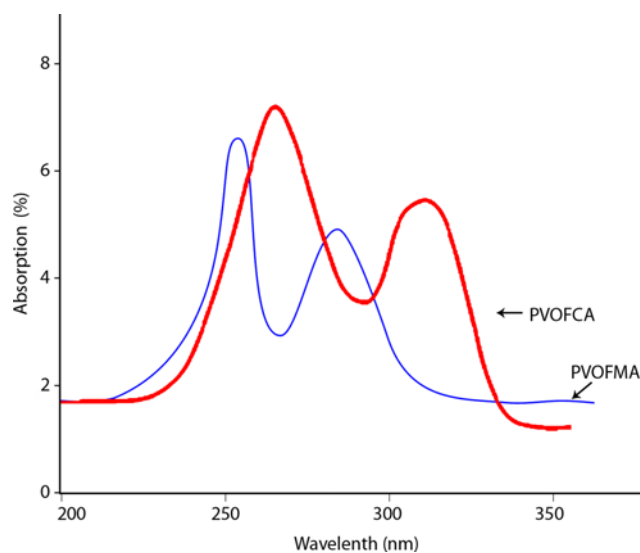


Fig. 3. UV-Vis spectra of (a) PVOFCA and (b) PVOFMA.

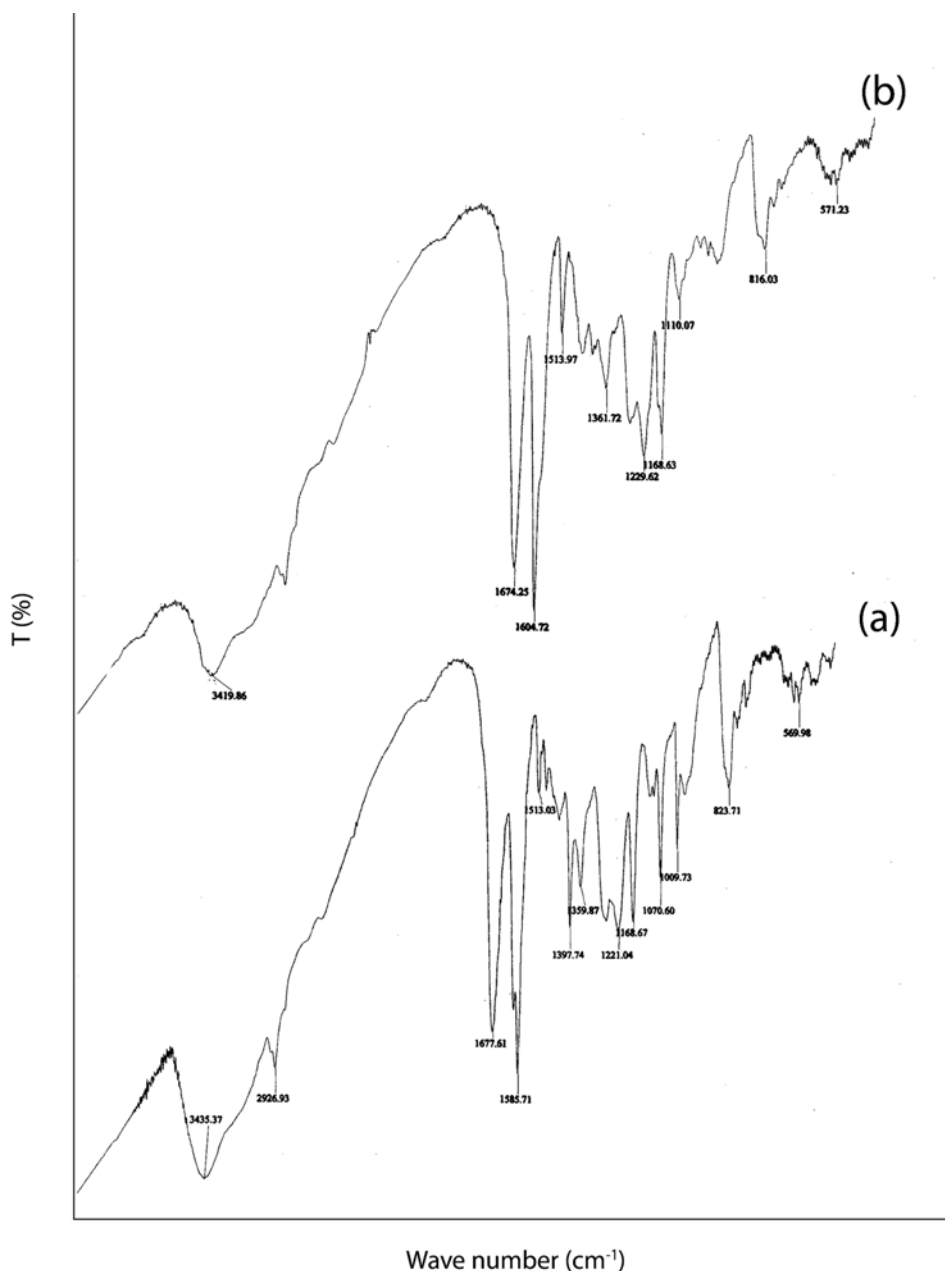


Fig. 4. FTIR spectra of (a) PVOFCA and (b) PVOFMA.

RESULTS AND DISCUSSION

1. UV-vis and FT-IR Analyses

The UV-visible spectra of terpolymers in pure DMSO were recorded in the region 190–360 nm (Fig. 3). Both terpolymers displayed two characteristic broad bands at 255 and 290 nm (PVOFMA) and at 265 and 315 (PVOFCA). These observed positions for absorption bands indicate the presence of a carbonyl ($>C=O$) group having a carbon oxygen double bond which is in conjugation with the aromatic nucleus. The bathochromic shift from the basic value, i.e., 250–320 nm, ($\Pi-\Pi^*$) and 270–300 nm ($>C=N$), may be due to the combined effect of conjugation (due to chromophore) and oxime hydroxy group (auxochrome).

The FT-IR spectra of both terpolymer resins are presented in Fig. 4. The characteristic broad bands at $3,435\text{ cm}^{-1}$ (VOFCA) and $3,420\text{ cm}^{-1}$ (VOFCA) are assigned to the hydroxyl group of oxime present in monomer moieties, which is due to intramolecular hydrogen bonding. The peaks observed at $2,926.9\text{ cm}^{-1}$ in VOFCA are due to C-H stretching vibration of aldoxime group. The characteristic peaks observed at $1,677.6\text{ cm}^{-1}$ in VOFCA and $1,674\text{ cm}^{-1}$ in VOFMA are due to C=N stretching of vanillin oxime moiety. The band at $1,513$ to $1,604\text{ cm}^{-1}$ is due to C-C stretching of the aromatic ring carbons. The O-H out-of-plane bending vibration gives rise to a broad band in the region 840 cm^{-1} . Appearance of a band at $1,361$ to $1,398\text{ cm}^{-1}$ is due to C-H stretching of methylene bridge between aromatic moieties. The medium band obtained at

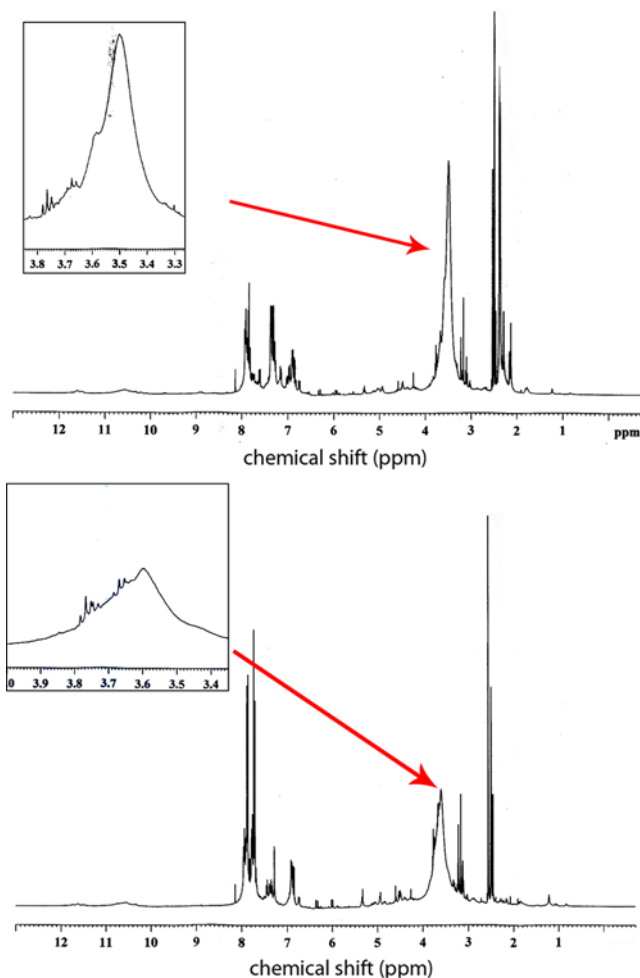


Fig. 5. ^1H NMR spectra of full and expanded form for (a) PVOFCA and (b) PVOFMA.

$1,110$ to $1,168\text{ cm}^{-1}$ suggests the $-\text{OCH}_3$ stretching. The 1, 3, 4, 5 tetra-substitution of aromatic benzene ring can be recognized at 816 and 823 cm^{-1} , for PVOFMA and PVOFCA, respectively.

2. NMR Analyses

The proton NMR spectra of terpolymer resins were scanned in $\text{DMSO}-d_6$ solvent. The spectra are depicted in Fig. 5. The chemical shift (δ) ppm observed is assigned on the basis of data available in literature. The terpolymer resin shows intense weakly multiplet signals at 2.4 (δ) ppm which may be attributed to methyl proton of $\text{Ar}-\text{COCH}_3$ group, whereas the signal at 2.5 is due to $\text{DMSO}-d_6$. The medium signal at 3.35 - 3.37 (δ) ppm may be due to methoxy proton of vanillin oxime moiety. The signal at 3.40 - 3.78 (δ) ppm may be due to the methylene proton of $\text{Ar}-\text{CH}_2-\text{Ar}$ moiety. The signal in the region 6.82 - 6.85 (δ) ppm is attributed to phenolic pro-

tons. The weak multiplet signal (unsymmetrical pattern) in the region of 7.2 - 7.8 (δ) ppm may be attributed to aromatic proton ($\text{Ar}-\text{H}$). The signal that appears at 8.2 (δ) ppm may be due to hydroxyl protons of aldoxime group. The position of the signal of protons of aldoxime group is slightly shifted to downfield, indicating clearly the intramolecular hydrogen bonding of $-\text{OH}$ group.

The ratio of monomer, comonomer and condensing unit in terpolymer resins was determined by ^1H NMR method [18]. It was determined by comparing the integrals (or intensity of signals) of methoxy (for VO unit), methylene backbone (for condensing unit) and methyl (for p-chloroacetophenone/p-methylacetophenone unit) region in the spectrum. Molar fractions of the comonomer units (m_1 , m_2 and m_3) in terpolymer resin using ^1H NMR analysis data were calculated according to the following equations:

$$\frac{A_{m1}(\text{OCH}_3)}{A_{total}} = \frac{n_1 m_1}{(a m_1 + b m_2 + c m_3)} \quad (6)$$

$$\frac{A_{m2}(\text{CH}_2)}{A_{total}} = \frac{n_2 m_2}{(a m_1 + b m_2 + c m_3)} \quad (7)$$

$$\frac{A_{m3}(\text{CH}_3)}{A_{total}} = \frac{n_3 m_3}{(a m_1 + b m_2 + c m_3)} \quad (8)$$

where A_{m1} , A_{m2} and A_{m3} are the normalized areas (or intensity) per H from the corresponding functional groups of the monomer unit regions; A_{total} is the total area of proton for carbon atoms in the terpolymer; n_1 , n_2 and n_3 are integers of proton(s) in the functional group of monomer units; a , b and c are the integers of proton in the monomer units; in the case of $(m_1 + m_2 + m_3) = 1$, monomer unit ratios can be calculated from Eq. (6) to (8) using the following simplified form:

$$\frac{m_1}{m_3} = \frac{n_3 A_{m1}(\text{OCH}_3)}{n_1 A_{m3}(\text{CH}_3)} \quad (9)$$

$$\frac{m_2}{m_3} = \frac{n_3 A_{m2}(\text{CH}_2)}{n_2 A_{m3}(\text{CH}_3)} \quad (10)$$

$$\frac{m_1 + m_2}{m_3} = \frac{n_3 [A_{m1}(\text{OCH}_3) + A_{m2}(\text{CH}_2)]}{(n_1 + n_2) A_{m3}(\text{CH}_3)} \quad (11)$$

The obtained results by ^1H NMR integral areas are summarized in Table 2.

3. Molecular Weight and Viscosity

The weight-average molecular weights (\overline{M}_w) and polydispersity indices ($\overline{M}_w/\overline{M}_n$) of terpolymer PVOFCA and PVOFMA are determined by GPC measurements and inherent viscosities by Ubbelohde viscometry. Obtained chromatograms and data are presented in Fig. 6 and Table 2. The inherent viscosities and molecular weight of PVOFMA were greater than that of PVOFCA. The polydispersity indices of PVOFMA and PVOFCA were found as 2.7 and 2.6,

Table 2. Physical properties of terpolymer resins

Terpolymer	Molar fractions from ^1H NMR			Molar mass and polydispersity indices by GPC			Viscosity mL/g
	m_1 (%)	m_2 (%)	m_3 (%)	\overline{M}_n ($\text{g}\cdot\text{mol}^{-1}$)	\overline{M}_w ($\text{g}\cdot\text{mol}^{-1}$)	$\overline{M}_w/\overline{M}_n$	
PVOFCA	1.23	0.92	0.42	4762	12,381	2.6	0.34
PVOFMA	1.29	0.84	0.68	5244	14,159	2.7	0.41

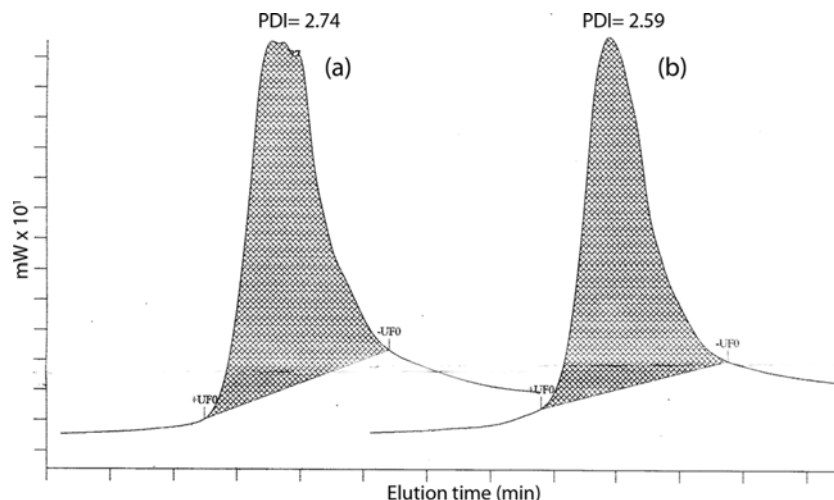


Fig. 6. GPC chromatogram of (a) PVOFCA and (b) PVOFMA.

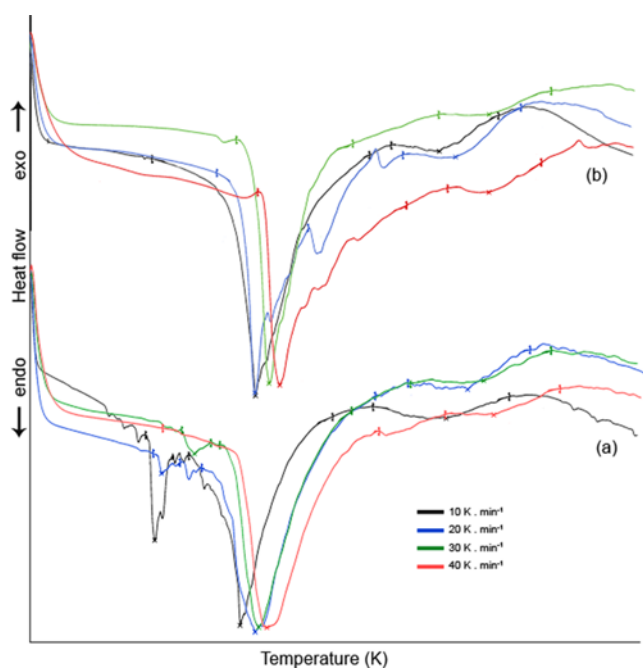


Fig. 7. Dynamic DSC thermograms at different heating rates (10, 20, 30, and 40 °C min⁻¹) for (a) PVOFCA and (b) PVOFMA.

respectively, which clearly suggests that terpolymerization proceeds through polycondensation mechanism.

4. DSC Analyses

The DSC thermograms at different scanning rate 10, 20, 30, and 40 °C/min are presented in Fig. 7. Characteristic (onset, endset and peak) temperatures and heat of melting ($H_{melting}$) in endotherms are shown in Table 3. As seen from data, DSC curves of both terpolymer resins showed two characteristic endo-peaks. The first broad endothermic transition at 102–140 °C (PVOFCA) and 105–134 °C (PVOFMA) corresponds to the expulsion of bound water (moisture). The water comes up by the quantity added during the synthesis of resin. The second endothermic peak at 163–218 °C (PVOFCA) and 165–215 °C (PVOFMA) is attributed to melting of resin system. It is known that the higher melting points of polymers are associated with many factors, including intramolecular interactions through hydrogen-bonded functional linkages between oxime and methylene linkage and structural regularity and rigidity of macromolecules. These results indicate that T_m significantly depends on the strong acidic vanillin oxime unit content in polymers. This allows proposing that the observed characteristic melt phase is the result of formation and melting of the strong hydrogen-bonded physically network structure. Tacticity also plays an important role on the thermal stability and the T_g of the terpolymer. The results indicated

Table 3. DSC thermogram data at different scanning rates

Terpolymer	Heating rate	First endotherm			Second endotherm		
		Temperature range (°C)	Peak temperature, T_p (°C)	Heat of melting (J/g)	Onset temperature T_{onset} (°C)	Peak temperature, T_p (°C)	Heat of melting (J/g)
VOFCA	10	101.8–120.1	105.7	67	163–192.3	181	5.7
	20	100–126	110	56	175–204	186.3	6.4
	30	103–130.3	111.9	66.7	175–210.6	194.4	7.6
	40	105.9–139.5	116	93.2	182.4–217.7	197.2	5.5
VOFMA	10	105–132	110.7	96.4	165–193	179.2	7.6
	20	108.2–118.3	112	40.4	169.8–203.4	185.7	8.4
	30	110–128.6	113.9	99.3	181.5–212	196.8	6.5
	40	114.7–134	119.6	66.6	185.3–214.5	196.9	2.94

Table 4. TG-DTG thermogram data at different scanning rates

Code	Heating rate °C/min	First endotherm	Second endotherm	Third endotherm		Fourth endotherm
				$T_{onset}-T_{endset}/T_d$ (°C)		
PVOFCA	10		134.6-178/154	-		478-500/519
	20	103.4-124/112.3	152.7-222/189	-		505.5-591/551
	30	101-123/110.9	131-257/169	-		522.9-601/563
	40	102.5-133/116.8	174.9-255.3/183	-		536-608/580
PVOFMA	10	-	164.6-201.8/183	-		529-548.5/531
	20	114.8-141/124	190-235.5/221	336-350/342.4		492.4-582/538
	30	107-132.9/117	206.7-255/226.2	347.7-366.6/357		514-592.9/559
	40	109-141.2/122	174-264/220	-		524-564.7/564

that the branching of the terpolymer chain was very pronounced or did have a significant effect on the T_g values [25].

Meanwhile, both terpolymer resins PVOFCA and PVOFMA show only T_g transitions at 102 °C and 107 °C, respectively, which indicates the amorphous structure of these compounds.

5. TG-DTG Analyses

Thermal properties were investigated by TG-DTG to assess the

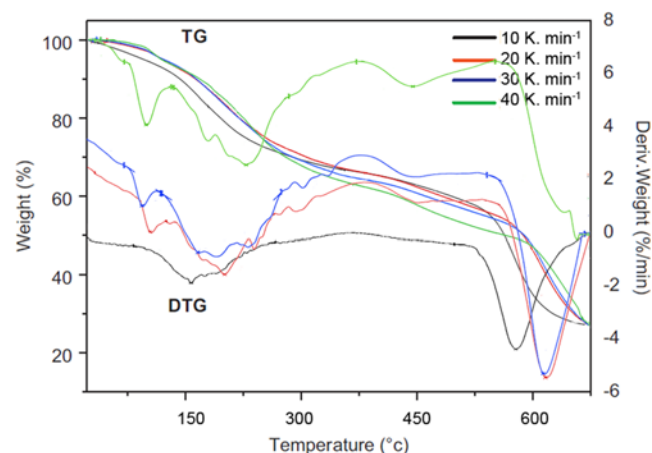


Fig. 8. TG-DTG plots obtained for PVOFCA in nitrogen atmosphere at different heating rates.

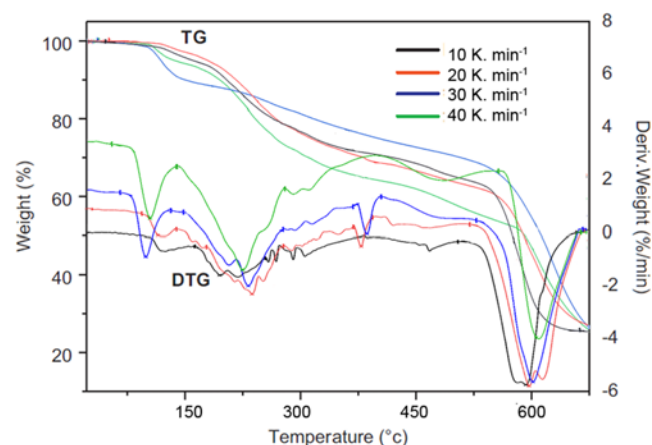


Fig. 9. TG-DTG plots obtained for PVOFMA in nitrogen atmosphere at different heating rates.

thermal stability of terpolymers. In Table 4, T_{onset} (the temperature at which the weight loss in the TGA curve begins), T_{endset} (the temperature at which the weight loss in the TGA curve completes), and T_d (the temperature at which the weight loss takes place at the highest rate) are reported. The thermograms TG-DTG of PVOFCA and PVOFMA at different heating (10, 20, 30 and 40 °C/min) are presented in Fig. 8 and 9, respectively. Terpolymer PVOFCA exhibits three-stage decomposition, whereas PVOFMA exhibits four-stage decomposition processes. The first stage (101-125 °C calculated; 95-130 °C theoretical) decomposition may be due to expulsion of bound water molecules present in the terpolymer. In the second stage, decomposition (135-225 °C calculated; 150-250 °C theoretical) corresponds to the loss of side group elimination attached to the aromatic nucleus, and final stage of decomposition (475-590 °C calculated; 450-600 °C theoretical) is probably due to main chain scission, which ultimately results in depolymerization into aromatic moieties. In terpolymer PVOFMA, an additional decomposition at 336-357 °C is due to strong ether linkage (Ar-CH₂-O-CH₂-Ar) which might be present during polycondensation process.

6. Kinetic Analysis

The apparent activation energy for the degradation of PVOFCA and PVOFMA was determined by two different model free kinetic (KAS and FRD) methods. The apparent activation energy values

Table 5. Activation energies data for different isoconversional methods

Degree of conversion	PVOFCA		PVOFMA	
	KAS method	Friedmann method	KAS method	Friedmann method
0.10	4.01	6.62	40.26	49.0
0.15	6.10	8.02	39.1	43.8
0.20	7.11	9.27	27.2	23.1
0.30	7.42	8.39	30.12	31.3
0.40	18.12	24.26	89.7	102.7
0.50	64.62	90.18	112.5	119.2
0.60	101	108.8	235.0	275.1
0.70	95.69	93.65	233.6	233.36
0.80	80.23	60.95	230.1	224.3
0.90	80.02	71.41	96.3	90.1
Mean	46.4	48.15	113.4	119.8

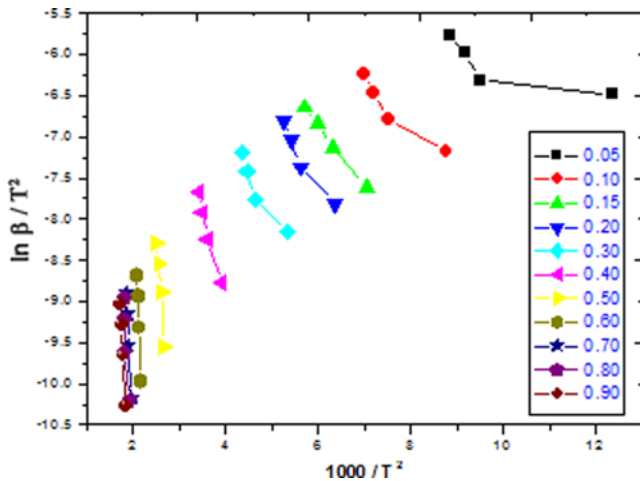


Fig. 10. Plots of $\ln(\beta/T^2)$ versus $1000/T$ of PVOFCA according to KAS method.

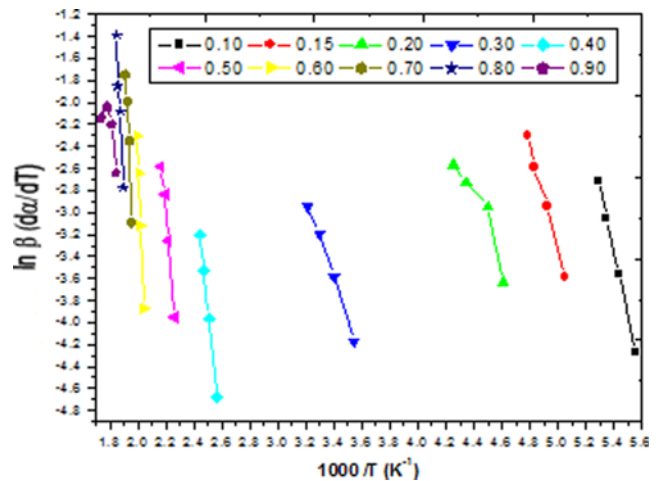


Fig. 13. Plots of $\ln(\beta \cdot d\alpha/dT)$ versus $1000/T$ according to FRD method of PVOFMA.

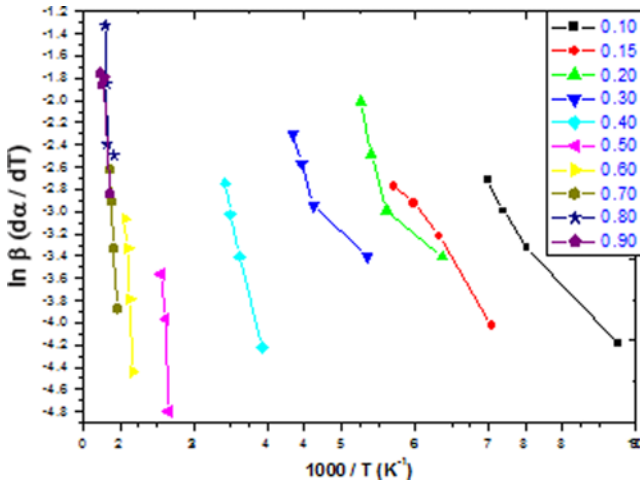


Fig. 11. Plots of $\ln(\beta/T^2)$ versus $1000/T$ of PVOFMA according to KAS method.

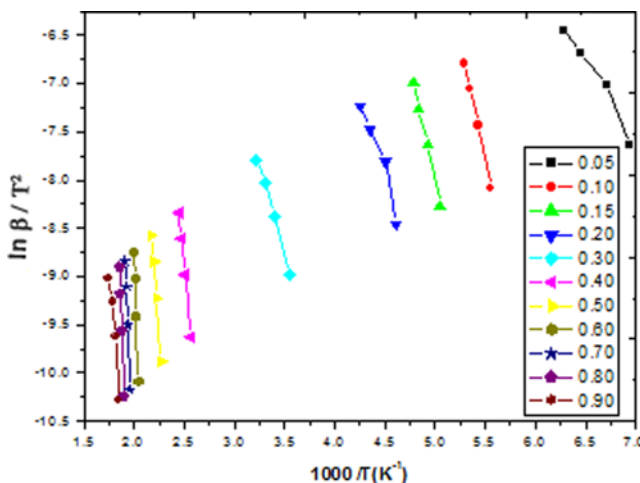


Fig. 12. Plots of $\ln(\beta \cdot d\alpha/dT)$ versus $1000/T$ according to FRD method of PVOFCA.

for the polymers by the mentioned two methods are in Table 5. The plots between the $\ln \beta/T^2$ and the $1000/T$ for PVOFCA and PVOFMA by KAS method are shown in Fig. 10 and Fig. 11, respectively. Similarly, the plots between the $\ln \beta(d\alpha/dT)$ and the $1000/T$ for FRD method for PVOFCA and PVOFMA by KAS method are presented in Fig. 12 and Fig. 13, respectively. The trends noted in the variation of apparent activation energy for the degradation of terpolymer obtained by KAS and FRD are different. This is due to the way in which the apparent activation energy was calculated, that is, KAS method is an integral method and FRD is a differential method. The change in apparent activation energy with respect to reaction extent for the KAS method leads to close values of E_a , but which differ substantially from the values of E_a obtained using iso-conversional method suggested by the Friedman method. The $Z(\alpha)$ - α master and experimental curve of the terpolymer PVOFCA and PVOFMA are presented in Fig. 14. The results show that the degradation follows Avrami-Erofeev (nucleation and growth) at initial stage to Jander (three-dimensional diffusion) model for PVOMAF and Jander (two-dimensional diffusion) for PVOFCA governed mechanisms.

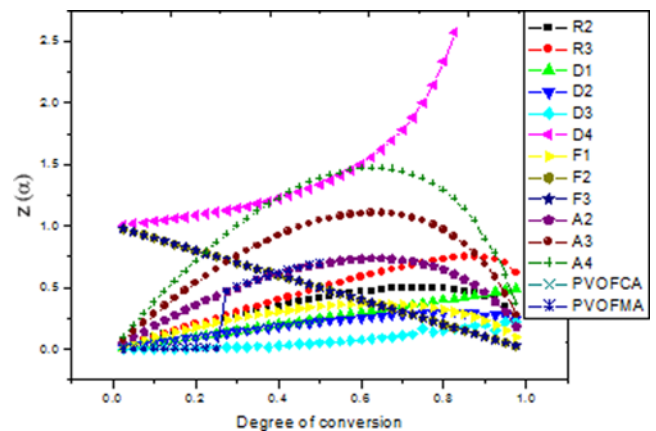


Fig. 14. Experimental master plots obtained from TG in the selected range of conversion represented versus the theoretical ones.

Table 6. Thermodynamic parameters for different terpolymers

Terpolymer code	ΔS^* (J)	G^* (kJ/mol)	k_r
PVOFCA	-37.5	27.8	4.8×10^{-3}
PVOFMA	-47.8	36.7	9.5×10^{-3}

By using data of TG and DTG analyses at 10 °C/min using KAS method, thermodynamic parameters like apparent entropy change (ΔS^*), free energy of activation (G^*) and reaction rate of activation (k_r) have been determined on the basis of thermal activation energy, using the equation below:

Entropy of activation (ΔS^*)

$$\Delta S^* = 2.303R \log \frac{Zh}{kT_d} \quad (12)$$

where K is Boltzmann constant, h is Planck constant and T_d is the peak temperature from DTG.

Free energy of activation (G^*)

$$G^* = E^* - T\Delta S^* \quad (13)$$

Reaction rate constant for activation (k_r)

$$k_r = Z e^{-E^*/RT_d} \quad (14)$$

The negative value of ΔS^* indicates that the activated complex has a more ordered structure than the reactants and further low values of Z indicate the slow nature of reaction.

By using data of thermogravimetric analysis, thermodynamic parameters like apparent entropy change (ΔS^*), free energy of activation (G^*) and reaction rate of activation (k_r) were determined on the basis of thermal activation energy are given in Table 6.

7. Antimicrobial Studies

Terpolymer resins were screened for antibacterial activity using the cup or well method technique. The minimum inhibitory concentration (MIC) represents the lowest concentration of antimicrobial agents at which point there is complete inhibition of organism growth. The minimum inhibitory concentration (MIC) was defined to be the intercept of the graph of logarithm concentration versus diameter of the inhibition zones. A lower MIC value is an indication of better antimicrobial agents. The MICs of the terpolymer resins were measured using a broth micro dilution method. 14-Well plates, contained in each well, a volume of 100 μ L of medium with a specific concentration of terpolymer (sequential two fold dilutions) was prepared. Each well was inoculated with 5 mL of culture (5×10^5 cells) and plates were incubated at 30 °C overnight. Controls of the medium were also carried out. MIC results were determined after 24 h of incubation. During the experiment it was observed that the extract, while preparing the dilutions and when added to the medium, formed a fine emulsion. Though a clear precipitate was not formed, the formation of emulsion indicated separation of nonpolar components of the extract in the aqueous medium. Since this may interfere with the availability of such components to the microorganisms and hence from exerting the activity, we modified the broth method, in which the medium containing the extract and the bacterial suspension was agitated in an orbital shaking incubator at 250 rpm. This is expected to effect an efficient mass transfer and bring the components of the extract in con-

Table 7. Antibacterial activity data for terpolymer resins and standard drugs

Compounds	Minimal inhibition concentration (μ g/mL)			
	<i>E. coli</i>	<i>P. aeruginosa</i>	<i>S. aureus</i>	<i>S. pyogenus</i>
PVOFCA	5	42	8	25
PVOFMA	12.5	60	50	35
Gentamycin	0.05	1	0.25	0.5
Amphicilin	100	100	250	100
Chloramphenicol	50	50	50	50
Ciprofloxacin	25	25	50	50
Norfloxacin	10	10	10	10

stant contact with the bacteria. This reduced the MIC considerably for all four bacteria tested. The antimicrobial activity of terpolymer resins was studied in different concentrations (5 μ g/mL, 25 μ g/mL, 50 μ g/mL, 100 μ g/mL) against four pathogenic bacterial strains (*E. coli* MTCC 442, *P. aeruginosa* MTCC 441, *S. aureus* MTCC 96 and *S. pyogenus* MTCC 443) and three fungal strains (*C. albicans* MTCC 227, *A. niger* MTCC 282 and *A. clavatus* MTCC 1323). The minimum inhibitory concentration of the antibacterial screening for these resins and standard drugs is presented in Table 7. From the results, it is clear that both of the terpolymer resins have shown reasonably good inhibitory activity against chosen bacteria as compared to very renowned standard drugs such as Gentamycin, Amphicilin, Chloramphenicol, Ciprofloxacin and Norfloxacin. The presence of chlorine in the resins has been assigned as the important component to prevent the growth of microorganisms [26]. Differences in MIC values of bacteria may be related to differential susceptibility of bacterial cell wall, which is the functional barrier to minor differences present in the outer membrane in the cell wall composition. The gram-positive and gram-negative microorganisms differ in several aspects other than with respect to the structure of their cellular walls, mainly with regard to the presence of lipoproteins and lipopolysaccharides in gram-negative bacteria that form a barrier to hydrophobic compounds [27]. This type of resin may have a mechanism of action similar to antimicrobial peptides as they may induce membrane permeation via membrane disintegration or pore formation, accompanied by a loss of bacterial membrane potential. The antibacterial mechanism of this cationic terpolymer disinfectant can be summarized in the following six steps [28]:

- Adsorption onto the bacterial cell surface
- Diffusion through the cell wall
- Binding to the cytoplasmic membrane
- Disruption of the cytoplasmic membrane
- It is possible that by the further action of the oxime, chloro hydroxyl and methoxy groups, and acetyl group intracellular contents are leaked, such as K^+ ions, DNA and RNA.
- Finally, the death of bacteria cells is led to probably.

Consequently, the overall activity is determined by two factors: one is favored for polymers (adsorption onto the bacterial cell surface, binding to the cytoplasmic membrane, and disruption of the cytoplasmic membrane), and the other is not favored for polymer (diffusion through the cell wall).

CONCLUSION

Novel terpolymer resins were synthesized in the presence of acid catalyst. The synthesized compounds were characterized by IR and ¹H NMR, GPC, viscosity, TG-DTG and DSC. All the synthesized compounds showed characteristic absorption peaks in IR and ¹H NMR spectra. DSC scans at different heating rates clearly demonstrated two-stage endothermic transition, which was probably due to expulsion of water and melting, respectively. Thermal degradation kinetics of both terpolymer resins was followed using two model free kinetic methods such as KAS and FRD. The apparent activation energy values for different conversions ($0.5 \leq \alpha < 0.90$) were found to be close to each other. The synthesized compounds were subjected to *in vitro* antibacterial evaluation. The antibacterial studies revealed that both terpolymer showed reasonably good activity due to functional groups like hydroxyl, oxime and chloro groups. This newly developed environmental friendly terpolymeric resin could be an exciting intermediate material for the construction of 3D-designed structural products.

ACKNOWLEDGEMENTS

Dr. N. P. S. Chauhan is thankful to his father A. S. Chauhan and Management, B. N. Institution for encouragement, HASETRI, JK Tyre, Rajsamand, SICART, Vallabh vidya nagar and CDRI, Lucknow for analytical and spectral data of terpolymer.

REFERENCES

1. H. Priefert, J. Rabenhorst and A. Steinbüchel, *Appl. Microbiol. Biotechnol.*, **56**, 296 (2001).
2. E. A. Borges-da-Silva, M. Zabkova, J. D. Araújo, C. A. Cateto, M. F. Barreiro, M. N. Belgacem and A. E. Rodrigues, *Chem. Eng. Res. Des.*, **87**, 1276 (2009).
3. A. Gandini, *Green Chem.*, **13**, 1061 (2011).
4. A. K. Sinha, U. K. Sharma and N. Sharma, *Int. J. Food Sci. Nutr.*, **59**, 299 (2008).
5. N. P. S. Chauhan, P. Kataria, J. Chaudhary and S. C. Ameta, *Int. J. Polym. Mater.*, **61**, 57 (2012).
6. N. P. S. Chauhan, *Des. Monomers Polym.*, **15**, 587 (2012).
7. F. S. Joseph, M. S. Joshua, J. L. S. John, H. R. Kaleigh and P. W. Richard, *Green Chem.*, **14**, 2346 (2012).
8. A. S. Amarasekara, B. Wiredu and A. Razzaq, *Green Chem.*, **14**, 2395 (2012).
9. G. P. Shulman and H. W. Lochte, *J. Appl. Polym. Sci.*, **10**, 619 (1996).
10. S. Vyazovkin, A. K. Burnham, J. M. Criado, L. A. Perez-Maqueda, C. Popescu and N. Sbirrazzuoli, *Thermochim. Acta*, **520**, 1 (2011).
11. S. Vyazovkin, *J. Comput. Chem.*, **22**, 178 (2001).
12. N. P. S. Chauhan, *J. Macromol. Sci. Pure Appl. Chem.*, **49**, 706 (2012).
13. F. Yao, Q. L. Wu, Y. Lei, W. H. Guo and Y. J. Xu, *Polym. Degrad. Stab.*, **93**, 90 (2008).
14. M. V. Alonso, M. Oliet, J. C. Dominguez, E. Rojo and F. Rodriguez, *J. Therm. Anal. Calorim.*, **105**, 349 (2011).
15. J. M. Perez and A. Fernandez, *J. Appl. Polym. Sci.*, **123**, 3036 (2012).
16. J. C. Dominguez, M. V. Alonso, M. Oliet, E. Rojo and F. Rodriguez, *Thermochim. Acta*, **498**, 39 (2010).
17. N. P. S. Chauhan and S. C. Ameta, *Polym. Degrad. Stab.*, **96**, 1420 (2011).
18. N. P. S. Chauhan, *J. Therm. Anal. Calorim.*, **110**, 1377 (2012).
19. N. P. S. Chauhan, *J. Macromol. Sci. Pure Appl. Chem.*, **49**, 655 (2012).
20. N. P. S. Chauhan, *J. Ind. Eng. Chem.*, **19**, 1014 (2013).
21. N. P. S. Chauhan, *Des. Monomers Polym.*, **17**, 176 (2014).
22. N. P. S. Chauhan, R. Ameta, S. C. Ameta, *J. Appl. Polym. Sci.*, **122**, 573 (2011).
23. J. Malek, *Thermochim. Acta*, **200**, 257 (1992).
24. N. Sbirrazzuoli, Y. Girault and L. Elegant, *Thermochim. Acta*, **249**, 179 (1995).
25. B. D. Iyer, I. A. Mathakiya, A. K. Shah and A. K. Rakshit, *Polym. Int.*, **49**, 685 (2000).
26. E. J. Lein, C. Hansch and S. M. Anderson, *J. Med. Chem.*, **11**, 430 (1968).
27. W. H. Zhao, Z. O. Hu, S. Okubo, Y. Hara and T. Shimamura, *Antimicrob. Agents Chemother.*, **45**, 1737 (2001).
28. B. G. Gottenbos, H. C. Van-der Mei, F. Klatter, P. Nieuwenhuis and H. J. Busscher, *Biomaterials*, **24**, 2707 (2003).